JMEPEG (2017) 26:4831–4837
DOI: 10.1007/s11665-017-2938-6

1059-9495/$19.00

Microstructure and Mechanical Properties of Mg-8Li-(0, 1, 2)Ca-(0, 2)Gd Alloys

Wei Miao, Chunbo Che, Kunning Fu, Ruizhi Wu, Legan Hou, Jinghuai Zhang, and Milin Zhang

(Submitted November 30, 2016; in revised form July 20, 2017; published online September 25, 2017)

A series of new Mg-8Li-*x*Ca-*y*Gd (*x* = 0, 1, 2; *y* = 0, 2; wt.%) alloys were prepared, and the microstructure and mechanical properties were investigated. The mechanical properties were characterized by tensile, compression and bending tests at room temperature. The results show that Mg-8Li-1Ca alloy is composed of alpha(Mg), beta(Li) and $CaMg_2$ phases. In addition to the same phases in Mg-8Li-1Ca, there also exists $CaLi_2$ phase in Mg-8Li-2Ca. In addition to the same phases in Mg-8Li-2Ca, $GdMg_5$ phase is also formed in Mg-8Li-1Ca-2Gd alloy due to the addition of Gd. Both Ca and Gd have refining effect in the alloys, and the refining effect of Ca is better than that of Gd. The additions of Ca and Gd can improve the tensile strength and yield strength, but decrease the elongation and the bending strength. Comparing the mechanical properties of the investigated alloys, Mg-8Li-1Ca-2Gd possesses the best mechanical properties.

Keywords calcium, gadolinium, grain refinement, magnesium-lithium alloys, mechanical property

1. Introduction

Mg-Li alloys are among the lightest metallic engineering materials and possess high specific strength, specific stiffness, good electromagnetic screen and superior shock resistance ability (Ref 1, 2).

Adding a small amount of lithium to magnesium can decrease the c/a ratio of the hexagonal closed-packed lattice of Mg. When Li addition is between 5.3 and 10.3 wt.%, a body-centered-cubic phase (BCC, β-Li phase) is introduced into hexagonal closed-packed Mg-based alloy (HCP, α-Mg phase), which results in the formation of ($\alpha + \beta$) duplex alloy. The formation of β-Li phase in Mg alloys can improve the ductility effectively but decrease the strength (Ref 3, 4). Great efforts have been made to enhance the comprehensive mechanical properties of Mg-Li alloys. Alloying is a common and effective method to improve mechanical properties (Ref 5, 6). A suitable amount of calcium addition has a good effect on grain refinement in Mg-Zr and Mg-Al alloys, causing the improvement of mechanical properties (Ref 7). In Mg-Gd-Zr alloy, with the addition of Ca content, the yield strength increases, and the elongation decreases (Ref 8). Rare earth (RE) elements can ameliorate the microstructure and enhance the mechanical properties effectively in Mg-Li alloys (Ref 9-11). Gd, as a heavy RE element, is beneficial for the improvement of both the mechanical properties and the corrosion resistance (Ref 12). A minor addition of Gd in Mg-Zn-Zr alloy can effectively refine grains and change phase compositions. The addition of Gd in as-rolled Mg-Zn-Zr alloy can effectively weaken the texture and modify the tensile fracture type from quasi-cleavage fracture to ductile fracture (Ref 13).

In this work, the as-cast Mg-8Li-*x*Ca-*y*Gd (*x* = 0, 1, 2; *y* = 0, 2; wt.%) alloys are prepared, and the influences of Ca and Gd on the microstructure and mechanical properties are investigated.

Wei Miao, Kunning Fu, Ruizhi Wu, Legan Hou, Jinghuai Zhang, and **Milin Zhang**, Key Laboratory of Superlight Materials and Surface Technology, Ministry of Education, Harbin Engineering University, Harbin 150001, People's Republic of China; and **Chunbo Che**, Key Laboratory of Superlight Materials and Surface Technology, Ministry of Education, Harbin Engineering University, Harbin 150001, People's Republic of China and Environment Engineering Department, College of Food Engineering, Harbin University of Commerce, Harbin 150076, People's Republic of China. Contact e-mail: ruizhiwu2006@yahoo.com.

2. Experimental Procedures

The investigated as-cast alloys were prepared by melting commercially pure (CP) Mg, CP Li, CP Ca and Mg—20 wt.% Gd master alloy in the melting furnace under the protective atmosphere of Ar. After melting, the melt was poured into a permanent mold. The book-shape as-cast ingots with dimensions of 230 mm × 145 mm × 40 mm were obtained. Then, the specimens for microstructure analysis and mechanical properties testing were cut from the ingot. The actual chemical compositions of the as-cast ingots measured by inductively coupled plasma analyzer (ICP, JY Ultima2) are listed in Table 1.

The specimens for microstructure observation were etched with a solution of 5 vol.% nital. The microstructures were observed by optical microscope (OM) and scanning electron microscope (SEM). The fracture microstructure was also observed by SEM. The phases of the alloys were analyzed by x-ray diffraction (XRD).

The tensile and compression tests were carried out on an electronic universal uniaxial testing machine. The initial strain rate during tensile tests was 1×10^{-3} s^{-1}, and the dimensions of the tensile specimen are shown in Fig. 1, in which the orientation of width, 15 mm, was parallel to the orientation of width, 40 mm, in the as-cast ingot. The compression specimens were cylinders, with dimensions of Φ 10 mm × 15 mm, in which the orientation of height, 15 mm, was parallel to the

Table 1 Actual chemical compositions of the four alloys, wt.%

	Li	Ca	Gd	Mg
Mg-8Li	7.88			Bal.
Mg-8Li-1Ca	8.21	1.11		Bal.
Mg-8Li-2Ca	8.14	1.78		Bal.
Mg-8Li-1Ca-2Gd	7.98	0.98	1.89	Bal.

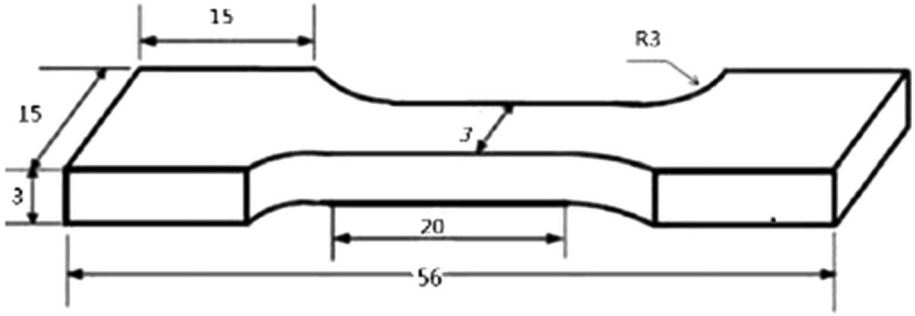

Fig. 1 Dimensions of specimen for tensile test

orientation of height, 145 mm, in the as-cast ingot. The compression rate was 1×10^{-3} s^{-1}. The dimensions of the three-point bending specimen were 30 mm × 18 mm × 3 mm, in which the orientation of length, 30 mm, is parallel to the orientation of width, 40 mm, in the as-cast ingot. The loading rate was 1.5×10^{-3} s^{-1}. During mechanical properties testings, all the test values were the average of at least three measurements.

3. Results and Discussion

3.1 Microstructure

Figure 2 shows the XRD patterns of the investigated alloys. Mg-8Li alloy is composed of α-Mg and β-Li. $CaMg_2$ phase appears in Mg-8Li-1Ca alloy. As the content of Ca increases to 2 wt.%, although the XRD peaks of $CaLi_2$ phase are not obvious, combined with the results of Fig. 3 and 4 and Ref 14, it can be deduced that there exists $CaLi_2$ phase in Mg-8Li-2Ca alloy. The solid solubility of calcium in magnesium is very small, less than 0.82%. When the content of Ca is larger than 0.82%, the excess Ca would react with Mg and Li to form new phases (Ref 14). After the addition of Gd, the amount of $CaMg_2$ and $CaLi_2$ phase decreases, and $GdMg_5$ phase appears. It is known that the larger electronegativity difference means an easier formation of the compound, and the compound is more stable. The electronegativity values of the four elements in the alloys are listed in Table 2. With the addition of Ca, it reacts with Mg to form Mg_2Ca preferentially because the electronegativity difference between Ca and Mg is larger than that between Ca and Li. When the content of Ca is large, Li_2Ca and Mg_2Ca both exist in the alloy. The solid solubility of Gd is much smaller in β-Li than that in α-Mg (Ref 15). Accordingly, although the electronegativity difference between Gd and Mg is less than that between Gd and Li, the supersaturated Gd preferentially reacts with Mg to form Mg-Gd compound in α-Mg matrix. The compound phases in this experiment are also consistent with the results of other literature (Ref 16-18).

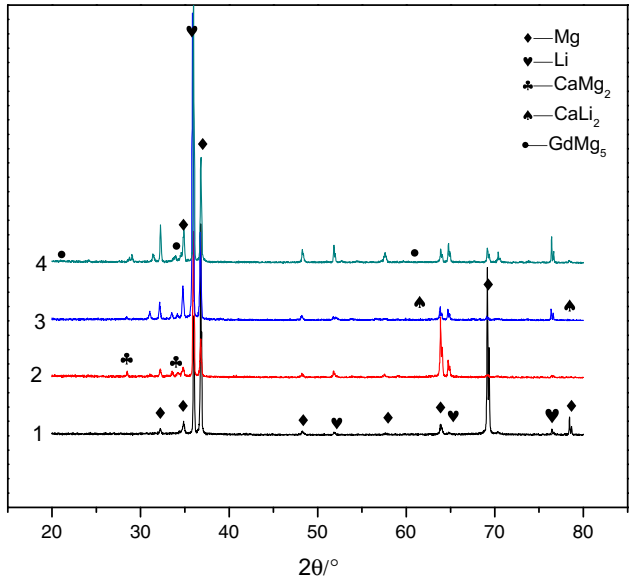

Fig. 2 XRD patterns of the investigated alloys 1—Mg-8Li; 2—Mg-8Li-1Ca; 3—Mg-8Li-2Ca; 4—Mg-8Li-1Ca-2Gd

Figure 3 shows the optical microstructures of the alloys. To observe the detailed microstructures, the high-magnification SEM images of Mg-8Li-2Ca and Mg-8Li-1Ca-2Gd alloys are shown in Fig. 4. In Mg-8Li alloy, the long-strip and blocky α-Mg phase is distributed in β-Li phase, as shown in Fig. 3(a) and (b). With the addition of 1 wt.% Ca, a network phase appears mainly at the phase boundaries between α-Mg and β-Li, as shown in Fig. 3(c) and (d). According to the XRD results of Fig. 2, the network phase is $CaMg_2$. When the content of Ca increases to 2 wt.%, the amount of $CaMg_2$ increases relatively. Additionally, many particles are uniformly distributed in β-Li phase, as shown in Fig. 3(e), (f), and 4(a). According to Ref 14, it can be concluded that this granular phase in Mg-8Li-2Ca alloy is $CaLi_2$. In Mg-8Li-1Ca-2Gd, the

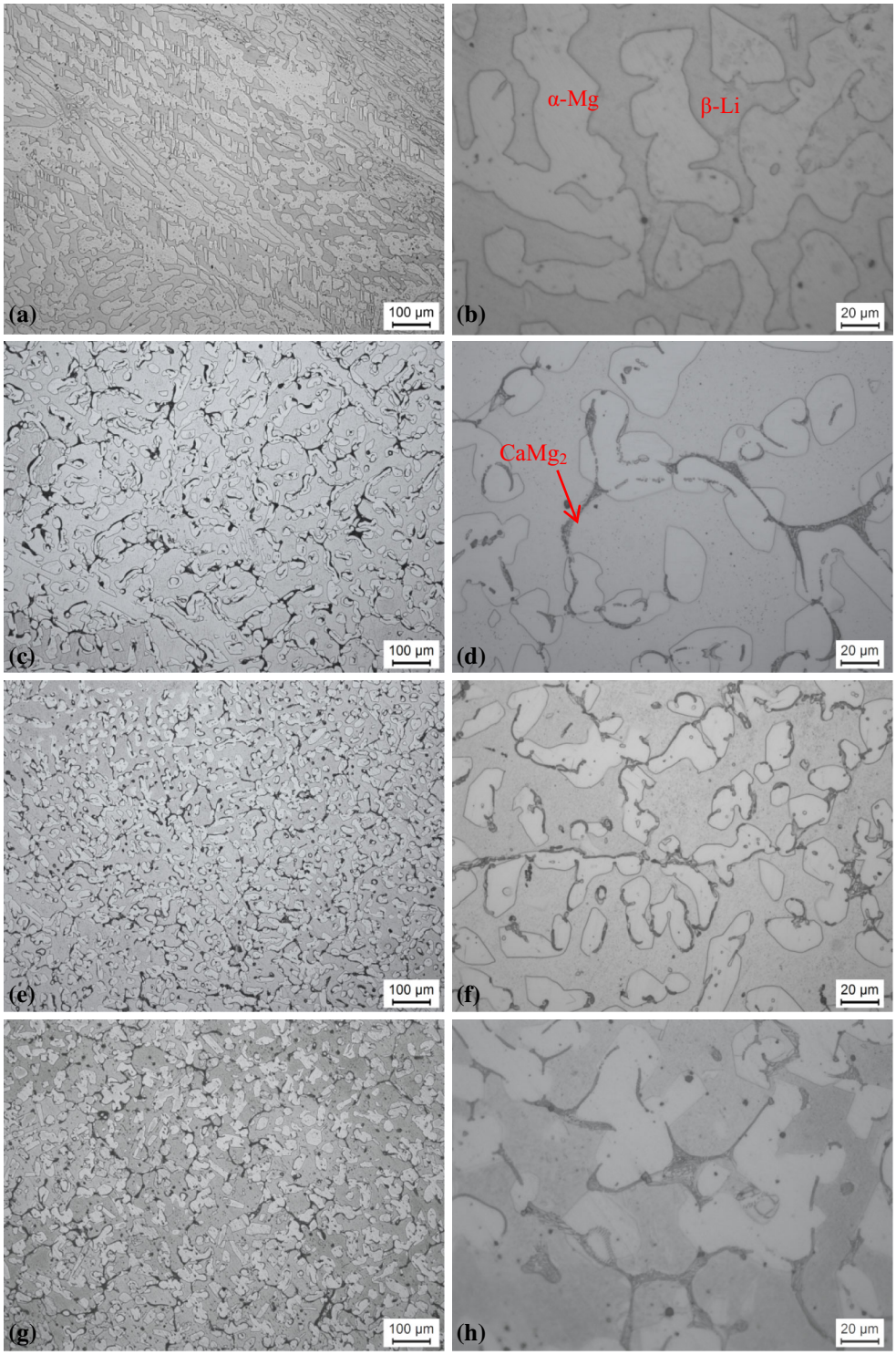

Fig. 3 Optical images of the investigated alloys (a, b) Mg-8Li; (c, d) Mg-8Li-1Ca; (e, f) Mg-8Li-2Ca; (g, h) Mg-8Li-1Ca-2Gd

amount of $CaMg_2$ phase is close to that in Mg-8Li-1Ca, and some white particles, whose size is larger than that of $CaLi_2$, appear in α-Mg and β-Li phases, as shown in Fig. 4(b). Combined with the XRD result, it can be concluded that the white granular phase in Fig. 4(b) is $GdMg_5$. Quantitatively analysis reveals that the percentages of $CaMg_2$ in Mg-8Li-1Ca, Mg-8Li-2Ca and Mg-8Li-1Ca-2Gd alloys are about 2.8 ± 0.2, 4.5 ± 0.3, and $2.6 \pm 0.2\%$, respectively. Comparing Fig. 3(d), (f), and (h), it can be observed that the size of $CaMg_2$ phase in Mg-8Li-2Ca is the finest, and that in Mg-8Li-1Ca-2Gd is the coarsest.

Quantitatively analysis indicates that the average α-Mg sizes of Mg-8Li, Mg-8Li-1Ca, Mg-8Li-2Ca and Mg-8Li-1Ca-2Gd are 30.5 ± 2.8, 25.3 ± 2.0, 15.5 ± 1.8, and 36.2 ± 3.1 μm, respectively. Comparing the microstructures of the four alloys, Ca and Gd both have refining effects in Mg-8Li alloy, and Mg-

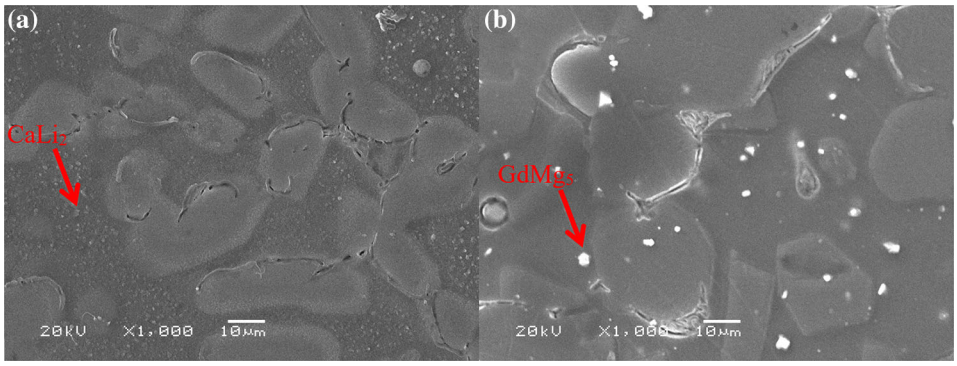

Fig. 4 SEM images of Mg-8Li-2Ca and Mg-8Li-1Ca-2Gd alloys (a) Mg-8Li-2Ca; (b) Mg-8Li-1Ca-2Gd

Table 2 The electronegativity of the four elements in the alloys

Elements	Mg	Li	Ca	Gd
Electronegativity	1.2	1.0	1.0	1.2

8Li-2Ca alloy possesses the finest microstructure. With the addition of Ca, Ca would segregate at the grain boundaries of α-Mg phase during the solidification, increasing the composition fluctuation (Ref 19). Therefore, the degree of supercooling increases, and the nucleation rate increases, causing the refining effects. Furthermore, $CaMg_2$ forms at the grain boundary and connects into a network, which also prevents the grain growth. Gd and Mg possess the same crystal structure (HCP) and similar lattice constants, and the melting point of $GdMg_5$ is higher than that of Mg. Therefore, during the solidification, $GdMg_5$ may serve as the heterogeneous nucleation, causing the grain refinement.

3.2 Tensile Properties

Figure 5 shows the stress–strain curves of the four alloys. The values of tensile strength (σ_b), yield strength ($\sigma_{0.2}$) and elongation (ε) are listed in Table 3. It can be found that the yield strength increases with the increase in Ca content. When the content of Ca is 1 wt.%, there is little effect on tensile strength of the alloy. The addition of 2 wt.% Ca is much more effective in the improvement of tensile strength. The addition of 2 wt.% Gd can further increase the strength, making Mg-8Li-1Ca-2Gd possesses the highest yield strength and tensile strength among the four alloys. The alloys with Ca or/and Gd possess much lower elongation values compared with Mg-8Li alloy. The elongation of Mg-8Li-1Ca is the minimum. Compared with Mg-8Li-1Ca and Mg-8Li-1Ca-2Gd, the elongation of Mg-8Li-2Ca is relatively high, which is about 2 times larger than that of Mg-8Li-1Ca.

In Mg-8Li-1Ca, the network $CaMg_2$ that exists at the phase boundaries between α-Mg and β-Li is a brittle compound. Although the microstructure of the alloy is refined because of Ca addition, the existence of large-size and brittle $CaMg_2$ makes the strengthening effect become unobvious and the ductility decrease seriously. When Ca content is 2 wt.%, the granular $CaLi_2$ phase appears in the alloy, making the amount of network $CaMg_2$ decrease and the refining effect become more obvious. Therefore, the strength and elongation of Mg-8Li-2Ca are both improved obviously compared with those of

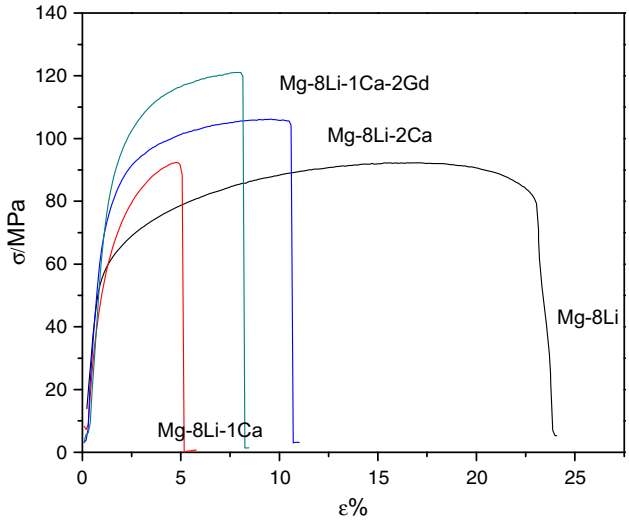

Fig. 5 Stress–strain curves of the alloys at room temperature

Mg-8Li-1Ca. Based on Mg-8Li-1Ca, adding 2 wt.% Gd leads to forming granular $GdMg_5$ and decreasing the amount of brittle network $CaMg_2$. What is more, the microstructure is further refined. Therefore, the strength is improved obviously. The strength of Mg-8Li-1Ca-2Gd is the highest among the four alloys. Because the amount of brittle network $CaMg_2$ in Mg-8Li-1Ca-2Gd alloy is somewhat larger than that in Mg-8Li-2Ca alloy, the elongation of Mg-8Li-1Ca-2Gd alloy is less than that of Mg-8Li-2Ca alloy.

Figure 6 shows the tensile fracture morphology of the alloys. There are a large number of deep dimples in the fracture of Mg-8Li alloy, showing a ductile fracture mode. There exist many cleavage planes, cleavage steps and obvious tear ridges in the fracture of Mg-8Li-1Ca, showing a quasi-cleavage mode. In Mg-8Li-2Ca alloy, cleavage planes and cleavage steps disappear, and small and shallow dimples appear, showing a type of mixed fracture mode. The network $CaMg_2$ phase distributing at phase boundary splits the matrix, causing a poor ductility. When Ca content increases to 2 wt.%, the dispersive $CaLi_2$ phase makes the ductility of the alloy increase. Compared with the fracture morphology of Mg-8Li-1Ca, due to the addition of Gd, the amount of cleavage planes, cleavage steps and tear ridges in the fracture of Mg-8Li-1Ca-2Gd decreases. The tensile fracture is a mixture of quasi-cleavage and tough dimple. With the addition of Gd, the grains are refined

Table 3 Tensile properties of the alloys

Alloys	$\sigma_{0.2}$, MPa	σ_b, MPa	ε, %
Mg-8Li	66.4 ± 2.1	92.0 ± 4.3	23.5 ± 0.31
Mg-8Li-1Ca	74.2 ± 3.2	92.4 ± 2.8	5.8 ± 0.5
Mg-8Li-2Ca	87.2 ± 2.6	105.9 ± 3.6	11.0 ± 0.29
Mg-8Li-1Ca-2Gd	95.7 ± 3.5	120.8 ± 2.5	8.1 ± 0.33

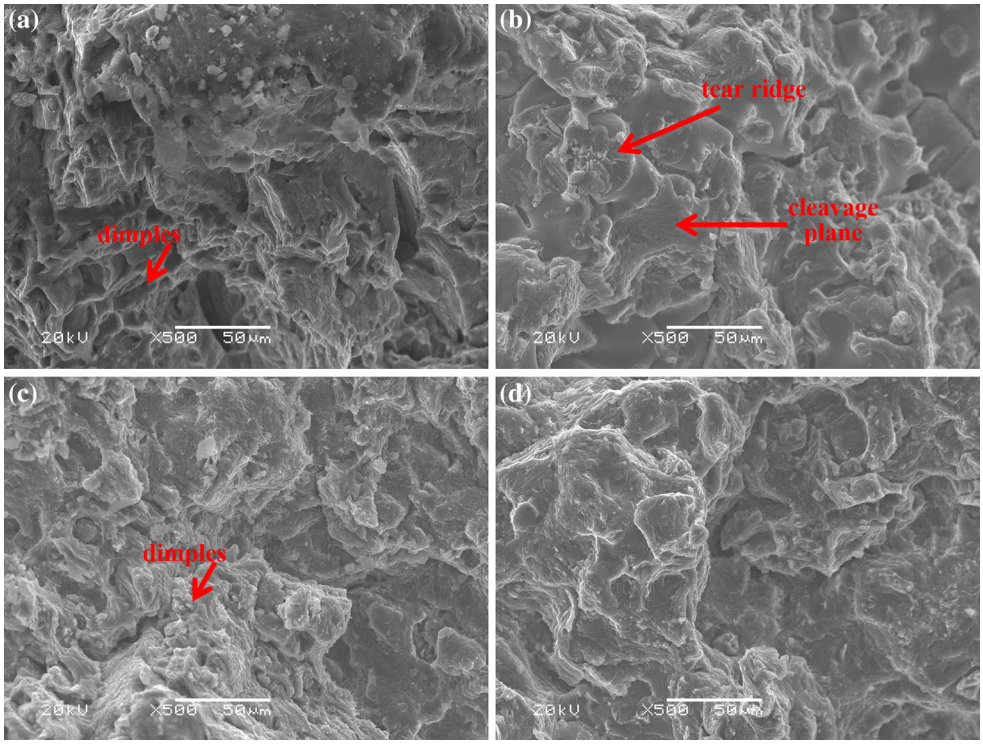

Fig. 6 Tensile fracture morphology of investigated alloys (a) Mg-8Li; (b) Mg-8Li-1Ca; (c) Mg-8Li-2Ca; (d) Mg-8Li-1Ca-2Gd

effectively. Furthermore, the formation of $GdMg_5$ phase makes the amount of brittle $CaMg_2$ phase decrease. As a result, the ductility of Mg-8Li-1Ca-2Gd is better than that of Mg-8Li-1Ca, which is consistent with results of stress–strain curves.

3.3 Compression Properties

During the compression process, all the specimens are not broken, only with a lot of small cracks on the surface. Figure 7 and 8 show the stress–strain curves and compressive yield strength of the four alloys. From Fig. 7, it can be found that the additions of Ca and Gd both increase the compressive yield strength. Mg-8Li-2Ca possesses the highest yield strength. Comparing the compressive strength values with the tensile strength values, it can be found that the addition of Ca performs more favorable effects on compressive strength than tensile strength. As for magnesium alloy, the deformation mechanism of compression is different from that of tensile. The piling up of dislocations during compression deformation is faster than that during tensile deformation (Ref 20). Compared with $GdMg_5$ phase in Mg-8Li-1Ca-2Gd, the size of particular $CaLi_2$ in Mg-8Li-2Ca is smaller and more uniform, and the distribution of it is more dispersive. The blocking effects of $CaLi_2$ particles on the dislocation movement are stronger (Ref 21). As a result, the compressive yield strength of Mg-8Li-2Ca is better than that of Mg-8Li-1Ca-2Gd.

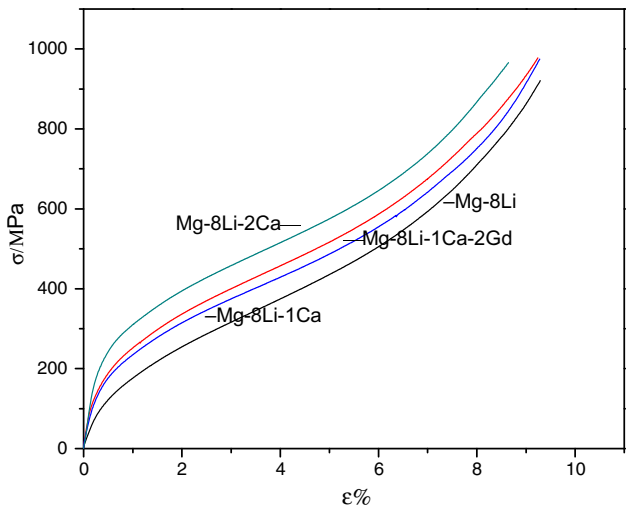

Fig. 7 Compressive stress–strain curves of alloys at room temperature

3.4 Bending Properties

Figure 9 shows the bending deformation curves of the four alloys. The bending strength of Mg-8Li is the highest. The

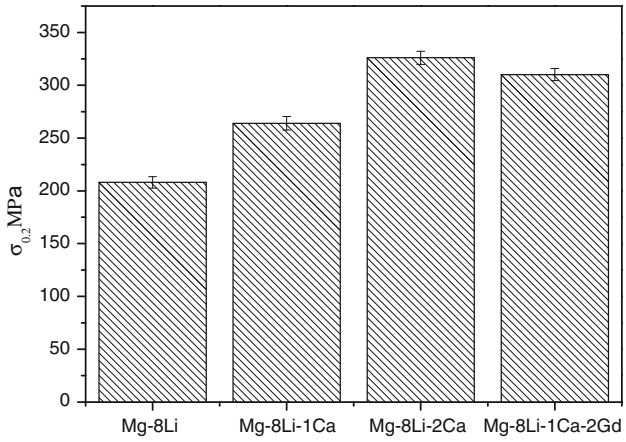

Fig. 8 Compressive yield strength of the alloys

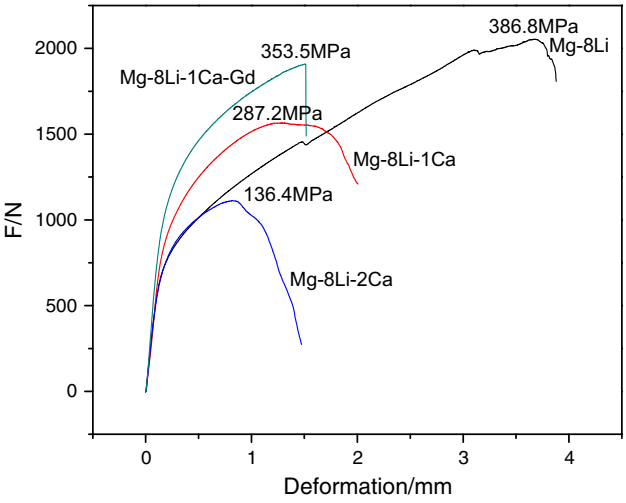

Fig. 9 Bending curves of the alloys at room temperature

formation of brittle $CaMg_2$ phase leads to the deterioration of bending strength. The dispersive $CaLi_2$ phase strengthens the matrix, and the strength and ductility are improved. Comparing the bending curves of the four alloys, it can be obviously found that the unfavorable effect of Gd on the bending strength is less than that of Ca. It can be attributed to the three factors caused by the addition of Gd, i.e., the decrease of brittle $CaMg_2$ phase, the formation of granular $GdMg_5$ phase and the refinement effect.

4. Conclusions

1. Mg-8Li-1Ca alloy is mainly composed of α-Mg, β-Li and $CaMg_2$. The network $CaMg_2$ phase distributes at the boundaries between α-Mg and β-Li. When Ca content increases to 2 wt.%, granular $CaLi_2$ phase forms in β-Li phases and the amount of network $CaMg_2$ phase decreases. Adding 2 wt.% Gd to Mg-8Li-1Ca alloy leads to the formation of granular $GdMg_5$ phase. The additions of Ca and Gd both have refining effect in the alloys, and the refining effect of Ca is better than that of Gd.
2. The additions of both Ca and Gd can increase the tensile strength, but decrease the elongation. The strengthening effect of Gd is better than that of Ca. The existence of network $CaMg_2$ is unfavorable for elongation. Compared with Mg-8Li-1Ca and Mg-8Li-1Ca-2Gd, Mg-8Li-2Ca possesses a relatively higher elongation.
3. The additions of Ca and Gd both increase the compressive yield strength. The addition of Ca performs more favorable effects on compressive strength than tensile strength. The strengthening effect of Ca is better than that of Gd. Mg-8Li-2Ca possesses the highest compressive yield strength.
4. The additions of Ca and Gd both make the bending strength deteriorate. The unfavorable effect of Gd on the bending strength is less than that of Ca.
5. Comparing the tensile strength, elongation, compression strength and bending strength, Mg-8Li-1Ca-2Gd possesses the best mechanical properties among the four alloys.

Acknowledgments

This paper was supported by National Natural Science Foundation (51671063), Research Fund for the Doctoral Program of Higher Education (20132304110006), the Fundamental Research Funds for the Central Universities (HEUCFG201703), Harbin City Application Technology Research and Development Project (2015AE4AE005, 2015RQXXJ001, 2016AB2AG013).

References

1. R.Z. Wu, Y.D. Yan, G.X. Wang, L.E. Murr, W. Han, Z.W. Zhang, and M.L. Zhang, Recent Progress in Magnesium-Lithium Alloys, *Int. Mater. Rev.*, 2015, **60**, p 65–100
2. G.B. Wei, Y. Mahmoodkhani, X.D. Peng, A. Hadadzadeh, T.C. Xu, J.W. Liu, W.D. Xie, and M.A. Wells, Microstructure Evolution and Simulation Study of a Duplex Mg-Li Alloy During Double Change Channel Angular Pressing, *Mater. Des.*, 2016, **90**, p 266–275
3. Y. Zeng, B. Jiang, D.H. Huang, J.H. Dai, and F.S. Pan, Effect of Ca Addition on Grain Refinement of Mg-9Li-1Al Alloy, *J. Magnes. Alloys*, 2013, **1**, p 297–302
4. R. Mahmudi, M. Shalbafi, M. Karami, and A.R. Geranmayeh, Effect of Li Content on the Indentation Creep Characteristics of Cast Mg–Li–Zn Alloys, *Mater. Des.*, 2015, **75**, p 184–190
5. T.L. Zhu, C.L. Cui, T.L. Zhang, R.Z. Wu, S. Betsofen, Z. Leng, J.H. Zhang, and M.L. Zhang, Influence of the Combined Addition of Y and Nd on the Microstructure and Mechanical Properties of Mg-Li Alloy, *Mater. Des.*, 2014, **57**, p 245–249
6. R.Z. Wu, Z.K. Qu, and M.L. Zhang, Effects of the Addition of Y in Mg-8Li-(1,3)Al Alloy, *Mater. Sci. Eng. A*, 2009, **516**, p 96–99
7. T. Wang, R.Z. Wu, M.L. Zhang, L. Li, J.H. Zhang, and J.Q. Li, Effect of Calcium on the Microstructures and Tensile Properties of Mg-5Li-3Al Alloys, *Mater. Sci. Eng. A*, 2011, **528**, p 5678–5684
8. L.L. Shi, Y.D. Huang, L. Yang, F. Feyerabend, C. Mendis, R. Willumeit, K.U. Kainer, and N. Hort, Mechanical Properties and Corrosion Behavior of Mg-Gd-Ca-Zr Alloys for Medical Applications, *J. Mech. Behav. Biomed.*, 2015, **47**, p 38–48
9. M.E. Moussa, M.A. Waly, and A.M. El-Sheikh, Effect of Ca Addition on Modification of Primary Mg_2Si, Hardness and Wear Behavior in Mg-Si Hypereutectic Alloys, *J. Magnes. Alloys*, 2013, **2**, p 230–238
10. F.A. Mirza, D.L. Chen, D.J. Li, and X.Q. Zeng, Effect of Rare Earth Elements on Deformation Behavior of an Extruded Mg-10Gd-3Y-0.5Zr Alloy During Compression, *Mater. Des.*, 2013, **46**, p 411–418
11. J. Zhang, Z. Leng, S. Liu, J. Li, M.L. Zhang, and R.Z. Wu, Microstructure and Mechanical Properties of Mg-Gd-Dy-Zn Alloy with

Long Period Stacking Ordered Structure or Stacking Faults, *J. Alloys Compd.*, 2011, **509**, p 7717–7722

12. X. Liu, Z.Q. Zhang, W.Y. Hu, Q.C. Le, L. Bao, and J.Z. Cui, Effects of Extrusion Speed on the Microstructure and Mechanical Properties of Mg-9Gd-3Y-1.5Zn-0.8Zr Alloy, *J. Mater. Sci. Technol.*, 2016, **32**, p 313–319
13. H.Y. Yu, H.G. Yan, J.H. Chen, B. Su, Y. Zheng, Y.J. Shen, and Z.J. Ma, Effects of Minor Gd Addition on Microstructures and Mechanical Properties of the High Strain-Rate Rolled Mg-Zn-Zr Alloys, *J. Alloys Compd.*, 2014, **586**, p 757–765
14. J. Gröbner, R. Schmid Fetzer, A. Pisch, C. Colinet, V.V. Pavlyuk, G.S. Dmytriv, D.G. Kevorkov, and O.I. Bodak, Phase Equilibria, Calorimetric Study and Thermodynamic Modeling of Mg-Li-Ca Alloys, *Thermochim. Acta*, 2002, **389**, p 85–94
15. H.W. Dong, L.D. Wang, Y.M. Wu, and L.M. Wang, Effect of Y on Microstructure and Mechanical Properties of Duplex Mg-7Li Alloys, *J. Alloys Compd.*, 2010, **506**, p 468–474
16. K. Suresh, K.P. Rao, Y.V.R.K. Prasad, N. Hort, and K.U. Kainer, Microstructure and Mechanical Properties of As-Cast Mg-Sn-Ca Alloys and Effect of Alloying Elements, *Trans. Nonferrous Met. Soc. China*, 2013, **23**, p 3604–3610
17. D.F. Zhang, X. Chen, F.H. Pan, L.Y. Jiang, G.S. Hu, and D.L. Yu, Research Progress of Effect of Rare Earth Elements on the Mechanical Properties of Magnesium Alloy, *Funct. Mater.*, 2014, **5**, p 5001–5007
18. G.S. Song and M.V. Kral, Characterization of Cast Mg-Li-Ca Alloys, *Mater. Charact.*, 2005, **54**, p 279–286
19. Y.Y. Zhou, L.P. Bian, G. Chen, L.P. Wang, and W. Liang, Influence of Ca Addition on Microstructural Evolution and Mechanical Properties of Near-Eutectic Mg-Li Alloys by Copper-Mold Suction Casting, *J. Alloys Compd.*, 2016, **664**, p 85–91
20. M.J. Mills and T. Neeraj, Dislocations in Metals and Metallic Alloys, *Encyclopedia of Materials: Science and Technology*, 2001, p 2278–2291
21. W. Zakulski, A. Debski, and W. Gasior, Enthalpy of Formation of the $CaLi_2$ Phase, *Intermetallics*, 2012, **23**, p 76–79